Rotational Dynamics of Transfer Ribonucleic Acid: Effect of Ionic Strength and Concentration†

John C. Thomas,* J. Michael Schurr, and Dennis R. Hare

ABSTRACT: We have investigated the influence of ionic strength and nucleic acid concentration on the rotational Brownian motion of *Escherichia coli* $tRNA_1^{Val}$ by studying the decay of the fluorescence polarization anisotropy (FPA) of intercalated ethidium on a nanosecond time scale. The rotational relaxation time τ_R remains essentially constant as the ionic strength is varied from 2 to 100 mM at a tRNA concentration of 54 mg/mL. τ_R also remains practically unchanged as the tRNA concentration is varied from 0.3 to 54 mg/mL at an ionic strength of 130 mM. Present hydrodynamic theories generally predict a more pronounced concentration dependence for rotational diffusion than we observe. This disagreement may result from a nonrandom distribution of the tRNA molecules in solution due to electrostatic interactions. By combining independent data from time-resolved nuclear Overhauser effect (NOE) cross-relaxation experiments and FPA experiments on the same tRNA, we are able to estimate the interproton spacing for the guanine N1-H and the uracil N3-H of the GU-50 base pair in *E. coli* $tRNA_1^{Val}$. This distance is 0.272 nm.

The present investigation was undertaken primarily to examine the rotational dynamics of tRNAs under conditions where long-range electrostatic interactions strongly perturb their spatial distribution. We also explicitly test the assumption common in NMR studies that very high tRNA concentrations have little effect on the rotational dynamics. In addition, the present data afford a partial test of existing theories of the concentration dependence of the rotational diffusion coefficients due to hydrodynamic interactions.

There exists ample evidence that highly charged macromolecules exhibit substantial ordering in dilute solutions of low ionic strength, where screening of their long-range electrostatic interactions is comparatively weak. In the case of charged polystyrene latex spheres, true long-range translational order has been demonstrated both by Bragg diffraction of visible light (Williams & Crandall, 1974; Williams et al., 1976; Crandall & Williams, 1977) and by direct microscopic examination (Kose et al., 1973; Ise et al., 1983a,b). In addition, the Young modulus (Williams et al., 1976; Crandall & Williams, 1977), shear modulus, and yield stress (T. Ohtsuki et al., unpublished results) of such arrays have been determined, and studies of the phase transition from liquidlike to solidlike states of such suspensions have been carried out (Hachisu et al., 1973; Takano et al., 1977; Schaefer et al., 1976; Ohtsuki et al., 1978). For much smaller ordinary polyions, such as flexible linear polyelectrolytes (Lin et al., 1978; Lee & Schurr, 1975; Shibata & Schurr, 1979; Martin et al., 1979; Plestil et al., 1979; Ise et al., 1980, 1983a,b; Moan et al., 1975, 1979; Cotton & Moan, 1976; Moan, 1978; Nierlich et al., 1978, 1979; Williams et al., 1979; Moan & Wolff, 1975; Rinaudo & Domard, 1977; Maret et al., 1979; Southwick et al., 1981), DNA fragments (Fullmer et al., 1981), tRNAs (Patkowski et al., 1980), nucleosomes (Schmitz, 1982; Schmitz et al., 1983, 1982), and bovine serum albumin (Giordano et al., 1981), various experiments manifest what appear to be related ordering phenomena at low salt concentrations, but conclusive evidence for true long-range order is lacking. The principal manifestations of ordering in these systems are (I) a transition to a weakly scattering extraordinary phase that exhibits a very small apparent diffusion coefficient in dynamic light scattering (DLS) (Lin et al., 1978; Lee & Schurr, 1975; Wilcoxon & Schurr, 1983), (II) one or more prominent maxima in the scattered intensity as a function of scattering vector in small-angle X-ray scattering (SAXS) (Plestil et al., 1979; Ise et al., 1980; Moan et al., 1975, 1979; Cotton & Moan, 1976; Moan, 1978; Nierlich et al., 1978, 1979; Williams et al., 1979; Moan & Wolff, 1975; Rinaudo & Domard, 1977; Ise et al., 1980, 1983a,b), and (III) a transition to cooperative alignment in magnetically induced birefringence experiments (Maret et al., 1979).

Recent tracer translational diffusion measurements (K. Zero and B. R. Ware, 1983; Ware et al., 1983) indicate that poly(L-lysine) molecules in the low-salt extraordinary phase move with almost undiminished mobility. This seems difficult to reconcile with any array exhibiting true long-range order or even multiple maxima in the intermolecular radial distribution function. Rotational ordering has been suggested as a possibility for nonspherical macromolecules (Lin et al., 1978; Martin et al., 1979), but no experimental data on the rotational dynamics of charged macromolecules under low-salt, strong-interaction conditions have been reported.

Electrostatic interactions in low-salt and salt-free $tRNA^{Phe}$ solutions have been investigated by SAXS, total intensity light scattering (ILS), and DLS by Patkowski et al. (1980). To account for their observations, which include multiple maxima in SAXS, reduced intensities in ILS, and very slow components in DLS, they propose the existence of ordered clusters. Here, we ask whether the same strong electrostatic interactions, which have a profound effect on SAXS, ILS, and DLS measurements, have a comparable effect on the rotational dynamics of a pure isoacceptor tRNA.

Considerable information regarding internuclear distances, especially interproton distances, is potentially available from time-dependent NOE, or magnetization transfer, experiments provided that the rotational dynamics of the tRNA are accurately known (Johnston & Redfield, 1981). Such structural information is part of the motivation for the large effort invested in assigning the various peaks in the proton spectrum (Johnston & Redfield, 1978; Hare & Reid, 1982a,b; Heershcap et al., 1983). It is commonly assumed that the rotational dynamics of the tRNA are unaffected by the

† From the Department of Chemistry, University of Washington, Seattle, Washington 98195. *Received February 7, 1984.* This work was supported in part by Grant GM29338-01 from the National Institutes of Health.

0006-2960/84/0423-5407$01.50/0

prodigious tRNA concentrations employed in NMR studies (≥50 mg/mL), but this has never been verified by an independent technique. We show below that that assumption is remarkably accurate.

Increasingly sophisticated theories of the effect of hydrodynamic interactions on the concentration dependence of the tracer rotational diffusion coefficient (D_R) of spherical species with stick boundary conditions have been developed. These can generally be expressed in the form

$$D_R = D_R^0(1 - K\phi) \quad (1)$$

to lowest order in the volume fraction ϕ of spheres. Here, $D_R^0 = k_BT/(8\pi\eta a^3)$ is the Debye result for spheres of radius a, and K is a theoretical coefficient. Wolynes & Deutch (1977) showed that inclusion of only the lowest order hydrodynamic interactions gave $K = 0$. Montgomery & Berne (1977) included the next higher order hydrodynamic interactions and obtained $K = {}^5/_{16}$. Freed & Muthukumar (1978) developed an effective medium theory that yields $K = 2.5$. The data presented below have sufficient precision to test some of these predictions.

In this study, we have made a series of determinations of the rotational relaxation time τ_R of *Escherichia coli* $tRNA_1^{Val}$ by measuring the decay of the fluorescence polarization anisotropy (FPA) of the ethidium bromide/$tRNA_1^{Val}$ complex on a nanosecond time scale. We have measured τ_R as a function of nucleic acid concentration over the range 0.3–54 mg/mL and as a function of ionic strength over the range 2–100 mM for a highly concentrated (54 mg/mL) solution.

Materials and Methods

tRNA Samples. The procedure used to purify the *E. coli* $tRNA_1^{Val}$ samples has been described previously (Reid et al., 1977) and is summarized here. Bulk, unfractionated tRNA from *E. coli* B was purchased from Plenum Scientific and subjected to chromatography on benzoylated DEAE-cellulose (Schwarz/Mann). The $tRNA_1^{Val}$ species was resolved from the later-eluting (1.02 M NaCl) Val-2A and Val-2B species on BD-cellulose chromatography. The early-eluting (0.73 M NaCl) 12-fold-purified Val-1 tRNA was purified to homogeneity by DEAE-Sephadex A-50 (Pharmacia) chromatography. For the studies of the ionic strength dependence of τ_R, the $tRNA_1^{Val}$ was microdialyzed into 2 mM NaCl, and the final $tRNA_1^{Val}$ concentration was 54 mg/mL. The monovalent salt concentration was increased to the desired value in the range 2–100 mM by adding aliquots of highly concentrated NaCl. For the measurements of τ_R as a function of nucleic acid concentration, the $tRNA_1^{Val}$ was microdialyzed into 100 mM NaCl containing 10 mM potassium phosphate (pH 7.0) so that the ionic strength was 130 mM. In this case, the $tRNA_1^{Val}$ concentration was varied by diluting the stock solution with the appropriate amount of dialysis buffer.

To each of the samples used in the FPA work was added ethidium bromide in the proportion of one ethidium per 100 $tRNA_1^{Val}$ molecules. This low ethidium concentration was used to ensure that substantial depolarization could not arise from energy transfer between neighboring ethidiums, to decrease the likelihood of having unbound ethidium in solution, and to ensure that only the primary ethidium binding site(s) would be occupied. For the NMR experiments, a 40 mg/mL solution of $tRNA_1^{Val}$ containing 50 mM NaCl, 10 mM potassium phosphate, and 1 mM Na_4EDTA (tetrasodium ethylenediaminetetraacetate) at pH 7.0 was used.

FPA Measurements. These measurements were carried out with a picosecond pulsed dye laser as the excitation source and time-correlated single-photon counting to detect the resultant ethidium fluorescence emission. The dye laser output consisted of 15 ps fwhm pulses at 575 nm, and the fluorescence emission beyond 630 nm was detected. A combination of polarizer, polarization rotator, and analyzer allowed selection of the fluorescence components with polarization parallel and perpendicular to the initial laser polarization. This system has been described previously in considerable detail (Thomas et al., 1980, 1984; Thomas & Schurr, 1983).

The sample was contained in a quartz cuvette, which in turn was enclosed in a jacketted housing. The temperature of the sample was maintained at 20.0 ± 0.1 °C by a VWR Model 90T water bath.

FPA Data Analysis. The experimental decay curves obtained are the sum or total fluorescence $s(t)$ and the difference between the two fluorescence polarization components $d(t)$. These measured data are actually convolutions of the instrument response function $e(t)$ and the true decay curves $S(t)$ and $D(t)$, respectively. A locally written nonlinear least-squares fitting routine using a convolute-and-compare method was used to determine the best-fit curves for $S(t)$ and $r(t) = D(t)/S(t)$. Here, $r(t)$ is the time-dependent fluorescence polarization anisotropy, which describes the Brownian rotational motion of the $tRNA_1^{Val}$/ethidium complex. $S(t)$ was modeled by a simple exponential decay (or a sum of exponentials).

In the most general case of a macromolecule with no symmetry properties, $r(t)$ will be a sum of five exponentials (Tao, 1969). In the less general case of an ellipsoid of revolution, $r(t)$ will consist of three exponential components, the relative amplitudes of which will depend on both the axial ratio of the ellipsoid and the ange between the transition dipole of the fluorescent probe and the symmetry axis of the ellipsoid. Assuming that tRNA can be reasonably described as a prolate ellipsoid with a suitable axial ratio, we have routinely attempted to fit $r(t)$ to a sum of exponentials plus a base line that could be fixed (e.g., at 0.0) or determined in the fitting process. All data analyses were carried out on a VAX 11/780 computer.

Time-Dependent NOE Measurements. Time-dependent NOE measurements were made with a Bruker WM500 pulsed FT NMR spectrometer at 32 °C. This instrument has been previously described (Hare & Reid, 1982a,b). In these experiments, the guanine N1-H of the GU-50 base pair (−11.4 ppm) in $tRNA_1^{Val}$ was saturated for varying periods of time, and the cross saturation to the N3-H of U-64 was observed. For monitoring the NOE buildup, we used preirradiation times of 50, 100, 150, 200, and 800 ms. The NOE data were collected directly by difference Fourier techniques. Alternate on-resonance and off-resonance pulses were accumulated with alternating memory negation to generate the difference free-induction decay (FID), which was then Fourier transformed to generate the difference spectrum in the frequency domain.

Time-Dependent NOE Data Analysis. The NOE data were reduced to a plot of integrated cross-saturation intensity (relative to the intensity of the saturated G-50 N1-H) vs. preirradiation time, and the initial slope of this curve was used as an estimate of the cross-relaxation rate σ_{ij} between the two adjacent protons. Assuming quasi-spherical top motion, σ_{ij} is related to the interproton distance r_{ij} and the rotational relaxation time τ_R of the tRNA by (Bothner-By, 1979)

$$\sigma_{ij} = \frac{\gamma^4[h/(2\pi)]^2}{10r_{ij}^6} \quad (2)$$

Here, γ is the proton gyromagnetic ratio, and h is Planck's constant. Thus, with the measured σ_{ij} we can estimate τ_R if

Table I: Concentration Dependence of the Fluorescence and Anisotropy Parameters for $tRNA_1^{Val}$ in 130 mM Ionic Strength Buffer

tRNA concn (mg/mL)[a]	ζ_R (nm)	fluorescence[b] a_1	τ_1 (ns)	a_2	τ_2 (ns)	anisotropy[c] r_0	τ_R (ns)	r_∞	D_R[d]
54.0 (2.04)	5.14	0.925 ± 0.01	25.09 ± 0.2	0.075 ± 0.01	7.54 ± 2.2	0.313 ± 0.01	23.05 ± 0.5	0.032 ± 0.02	7.23
3.0 (0.113)	13.47	0.921 ± 0.01	25.44 ± 0.2	0.079 ± 0.01	5.63 ± 1.4	0.324 ± 0.02	24.10 ± 0.8	0.050 ± 0.004	6.92
0.3 (0.011)	29.02	0.914 ± 0.01	25.65 ± 0.2	0.086 ± 0.01	5.61 ± 0.9	0.341 ± 0.004	24.41 ± 0.8	0.057 ± 0.009	6.83

[a] The $tRNA_1^{Val}$ concentration in millimoles per liter is shown in parentheses. [b] $S(t) = a_1 (\exp(-t/\tau_1) + a_2 \exp(-t/\tau_2)$. $a_1 + a_2 = 1.0$. [c] $r(t) = r_0 \exp(-t/\tau_R) + r_\infty$. [d] D_R is the equivalent sphere rotational diffusion coefficient calculated from eq 5. Units are 10^6 rads squared per second.

Table II: Ionic Strength Dependence of the Fluorescence and Anisotropy Parameters for $tRNA_1^{Val}$ at 54 mg/mL

[NaCl] (mM)	κ^{-1} (nm)[a]	fluorescence[b] a_1	τ_1 (ns)	a_2	τ_2 (ns)	anisotropy[c] r_0	τ_R (ns)	r_∞	D_R[d]
2	6.7	0.912 ± 0.02	25.81 ± 0.2	0.088 ± 0.02	9.89 ± 1.7	0.306 ± 0.02	22.30 ± 0.5	0.052 ± 0.007	7.47
2	6.7	0.926 ± 0.007	25.59 ± 0.1	0.074 ± 0.007	8.05 ± 1.5	0.317 ± 0.01	22.58 ± 0.5	0.051 ± 0.004	7.38
10	3.0	0.944 ± 0.06	25.27 ± 0.06	0.056 ± 0.004	6.48 ± 0.7	0.310 ± 0.009	22.78 ± 0.3	0.021 ± 0.009	7.32
42	1.47	0.942 ± 0.008	25.34 ± 0.03	0.058 ± 0.008	7.84 ± 0.48	0.326 ± 0.01	22.20 ± 0.44	0.033 ± 0.004	7.51
100	0.95	0.925 ± 0.01	25.09 ± 0.2	0.075 ± 0.01	7.54 ± 2.2	0.313 ± 0.01	23.05 ± 0.5	0.032 ± 0.02	7.23

[a] κ^{-1} is the Debye screening length. [b] $S(t) = a_1 \exp(-t/\tau_1) + a_2 \exp(-t/\tau_2)$. $a_1 + a_2 = 1.0$. [c] $r(t) = r_0 \exp(-t/\tau_R) + r_\infty$. [d] D_R is the equivalent sphere rotational diffusion coefficient calculated from eq 5. Units are 10^6 rads squared per second.

a good value for r_{ij} can be found.

Results

Figure 1 shows a typical data set from the FPA experiment along with the best-fit curves on a time scale of 0.0792 ns/channel. Figure 1A is a plot of the sum data $s(t)$ along with the best fit double exponential [convoluted with the instrument response function $e(t)$]. Also shown on the figure is a plot of the residuals between the experimental data and the fitted curve. Visual examination of the plot reveals that the best fit curve fits the experimental data extremely well. This is further supported by the fact that the residuals are evenly distributed about zero and show no systematic variation. Furthermore, the reduced χ_r^2 value of 1.17 is close to the value of 1.0, which is expected when the functional form is a good representation of the data and when the standard deviation of the data is known independently as it is in this case of simple Poisson photon statistics (Bevington, 1969).

In Figure 1B we show the difference data $d(t)$ and the best fit curve, which in this case is found by modeling $r(t)$ with a single exponential plus a free base line, i.e.

$$r(t) = r_0 \exp(-t/\tau_R) + r_\infty \qquad (3)$$

Here, r_0 and r_∞ are respectively the amplitude and base line and are determined in the fitting process. Attempts to fit these data with either a single or multiple exponentials with the base line set to zero inevitably failed. Again, we see that the experimental data are fitted well by the best fit curve, that the residuals are scattered evenly about zero with no obvious systematic variation, and that the reduced χ_r^2 value of 1.17 is indicative of a good match between the best fit curve and the experimental data.

Table I gives a summary of the best-fit parameter values for the fluorescence and the anisotropy obtained for $tRNA_1^{Val}$ solutions at three nucleic acid concentrations. The mean distance ζ_R between the molecules, assuming a random distribution, is also tabulated as a function of concentration. These values are calculated from the relationship $\zeta_R = 0.55n^{-1/3}$ (Chandrasekhar, 1943). Here, n is the number of molecules per unit volume. In Table II we show the variation of these best fit parameters with NaCl concentration over the range 2–100 mM for $tRNA_1^{Val}$ at a concentration of 54 mg/mL. The parameter values given are the average of five experimental data sets like the one shown in Figure 1. The uncertainty is the standard deviation obtained from the five

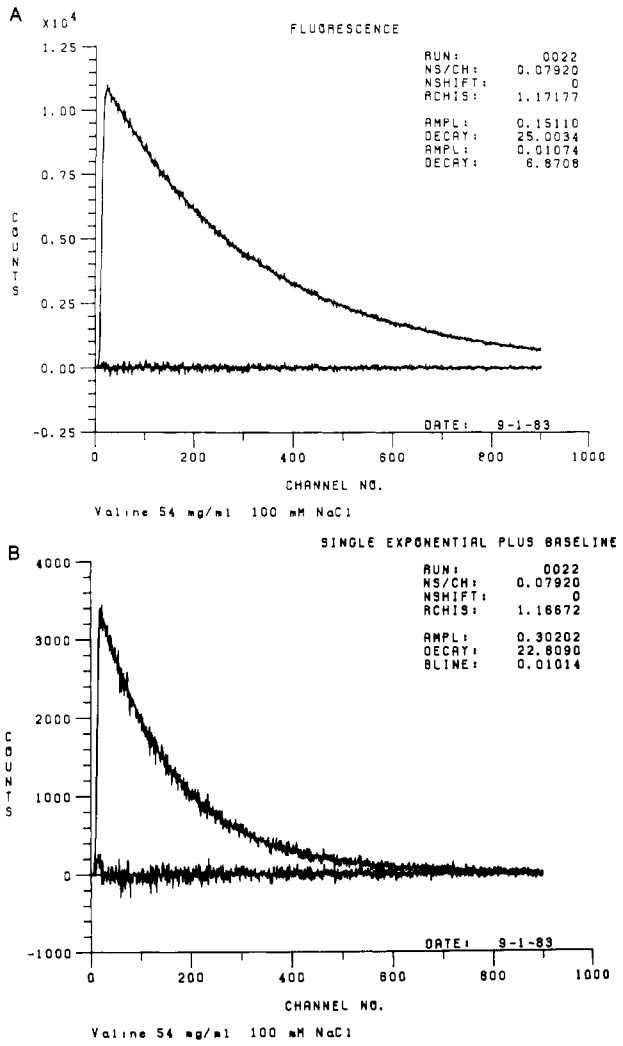

FIGURE 1: (A) Experimental sum fluorescence response $s(t)$ for ethidium/$tRNA_1^{Val}$ on a time scale of 0.0792 ns/channel. The data are fitted to the form $s(t) = \int_0^t e(t)S(t - t')\,dt'$. Here, $e(t)$ is the instrument response function, and $S(t)$ is the true fluorescence decay signal that was modeled by two exponentials. tRNA concentration is 54 mg/mL, ethidium bromide is 1%, and the solution ionic strength is 130 mM. (B) experimental difference data $d(t)$ corresponding to the fluorescence data shown in (A). The best fit curve is obtained by fitting the data to a convolution of the form $d(t) = \int_0^t e(t)S(t - t')r(t - t')\,dt'$. Here, $e(t)$ is the instrument response function, $S(t)$ is the fluorescence decay [obtained from (A)], and the anisotropy $r(t)$ is modeled by a single exponential plus a free base line.

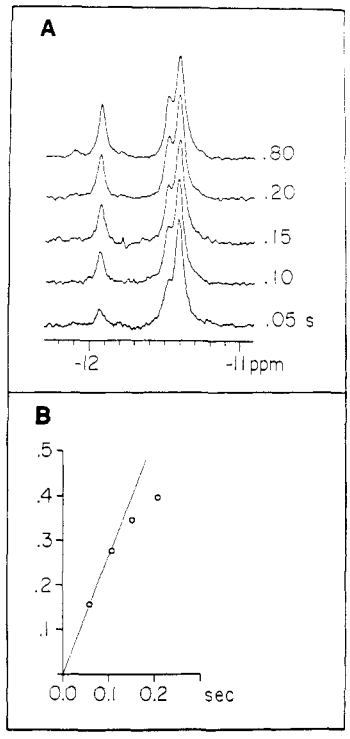

FIGURE 2: Time-dependent NOE data resulting from saturating the G N1-H of GU-50 (−11.4 ppm) in $tRNA_1^{Val}$ for varying periods of time. The N3-H of U-64 (−11.93 ppm) is cross saturated by the N1-H proton of G-50. (A) The 500-MHz difference spectra for the different preirradiation times. (B) Integrated cross-relaxation intensity as a function of preirradiation time.

different data sets. The Debye screening length κ^{-1} is also shown for each ionic strength.

Figure 2 summarizes the time-dependent NOE results. Part A shows the time dependence of the NOE between the G-50 N1-H and the U-64 N3-H of the base pair, and part B is a plot of the integrated cross-relaxation intensity vs. preirradiation time for the spectra shown in part A. The initial rate of the cross relaxation is shown by the line passing through the origin and the first two points. Note that after ~100 ms the rate decreases because the partially saturated N3-H is itself beginning to relax through nearby protons. The initial slope of the curve gives a cross-relaxation rate $\sigma_{ij} = 2.53\ s^{-1}$.

Discussion

Effect of Nucleic Acid Concentration in 130 mM Ionic Strength Buffer. (*a*) *Fluorescence Decay.* For all samples, the fluorescence decayed in a biexponential fashion and was well fitted by the relation

$$S(t) = a_1 \exp(-t/\tau_1) + a_2 \exp(-t/\tau_2) \qquad (4)$$

It can be seen from Table I that both the normalized amplitudes a_1 and a_2 and the corresponding lifetimes τ_1 and τ_2 show only a slight variation with $tRNA_1^{Val}$ concentration. Linear extrapolation of these data to zero $tRNA_1^{Val}$ concentration yields $a_1^0 = 0.917$, $\tau_1^0 = 25.56$ ns, $a_2^0 = 0.083$, and $\tau_2^0 = 5.56$ ns.

The observation of two fluorescence lifetimes is unequivocal evidence of *at least* two ethidium binding sites on $tRNA_1^{Val}$. The majority component lifetime $\tau_1^0 = 25.56$ ns is close to the value 22 ns, which we measure for ethidium intercalated with ϕ29 DNA (Thomas et al., 1980; Thomas & Schurr, 1983). We conclude therefore that the major component is the result of fluorescence emission from a fully intercalated ethidium molecule. The other lifetime $\tau_2^0 = 5.56$ ns is too short to arise from a truly intercalated ethidium, yet it is substantially longer than 1.5 ns, which is the lifetime that we measure for free ethidium in water at 20 °C. The intermediate length of the second lifetime suggests that it emanates from an ethidium that is attached to an area of the tRNA where it is less well shielded from the solvent than it would be in a true intercalation site.

Solution studies of the interaction between ethidium bromide and yeast $tRNA^{Phe}$ indicate that ethidium occupies an intercalation site in the acceptor stem between the U-6–A-67 and U-7–A-66 base pairs (Wells & Cantor, 1980). Conversely, crystallographic studies suggest that ethidium locates in the P_{10} cavity (Liebmann et al., 1977). This is evidence that there are at least two binding sites for ethidium on $tRNA^{Phe}$ and further that the affinity of these sites depends on the degree of hydration. The P_{10} cavity is an open region in the knee of the tRNA so that if an ethidium were located there we would expect that, compared with a true intercalation site, the increased solvent access would more fully quench the fluorescence and decrease the fluorescence lifetime. These considerations lead us to suggest that the two fluorescence components that we observe arise from a large population of tightly intercalated ethidium (giving the 25.56-ns component) and a much smaller population of ethidium hydrogen bonded in the P^{10} cavity (giving the 5.56-ns component).

Tao et al. (1970) have made fluorescence lifetime measurements of ethidium bromide bound to yeast $tRNA^{Phe}$ with and without magnesium. In the presence of magnesium (38 Mg^{2+} per tRNA molecule), they found also that the fluorescence was biphasic with lifetimes of 25.6 and 11 ns contributing 85 and 15% of the total, respectively. With no magnesium present, they found the fluorescence decay to be a single exponential with a lifetime of 26.2 ns. Although our samples have no added Mg^{2+}, we took no steps to remove the endogenous Mg^{2+} so each tRNA molecule would have had several Mg^{2+} associated with it. In the experiments of Tao et al. (1970) the raw data were not deconvoluted, and as the authors acknowledge, this could lead to small errors in their measurements. Those experiments also suffered from lower time resolution than the present work. In view of these differences, our results for $tRNA_1^{Val}$ are in reasonable accord with the results for $tRNA^{Phe}$ obtained by Tao et al. (1970).

(*b*) *Fluorescence Polarization Anisotropy.* As shown in Figure 1B, $d(t)$ was fitted best when the anisotropy was modeled by a single exponential plus a free base line. This result is somewhat surprising on two accounts. First, as discussed above, for an ellipsoid of revolution we expect that $r(t)$ may contain up to three exponential decay components, yet we detect only one component. Tao et al. (1970) also detected only one component in nanosecond depolarization studies of ethidium/$tRNA^{Phe}$. They pointed out that a single decay component would be observed if either (a) the tRNA was very nearly spherical in shape or (b) the tRNA could be described by a prolate ellipsoid of revolution with an axial ratio of 2 or 2.5 (corresponding to an angle of 0 or 40° between the ethidium transition dipole and the ellipsoid symmetry axis, respectively).

The second point that deserves comment is the base-line contribution to $r(t)$. Such a base-line contribution normally only arises in the case of restricted rotation (e.g., a fluorophore in a bilayer membrane). Under the present circumstances, the $tRNA_1^{Val}$ molecules should be quite free to rotate so that $r(t)$ would be expected to decay all the way to zero. It is possible that a small fraction of the tRNA is present in very slowly rotating aggregates, but we have no independent evidence of that. At present, we are not able to offer a more

concrete explanation for the nonzero base line.

The anisotropy parameters exhibit a remarkably slight concentration dependence. Extrapolation of the anisotropy decay time τ_R to zero concentration gives $\tau_R^0 = 24.3 \pm 0.6$ ns at 20 °C. This time, which we identify with the rotational relaxation time of $tRNA_1^{Val}$, is somewhat smaller than the value 28 ns (corrected to 20 °C) obtained by Tao et al. (1970) for yeast $tRNA^{Phe}$ at a concentration of 1.8 mg/mL. We have found previously (Thomas et al., 1984) that yeast $tRNA^{Phe}$ and *E. coli* $tRNA_1^{Val}$ have essentially identical rotational relaxation times in the presence of endogenous Mg^{2+} so that the small difference between the result of Tao et al. (1970) and the present result is probably due to the previously mentioned differences between the two experiments. We have found that the value obtained for the anisotropy relaxation time depends somewhat on how well the experimental data are deconvoluted. As Tao et al. (1970) did not deconvolute their data, it is difficult to make an absolute comparison with their results, but as was found for the fluorescence lifetimes, there is essential agreement between the two sets of results.

Estimating τ_R from the NOE cross-relaxation data is a treacherous affair due to the sixth-power dependence shown in eq 2. A small error in the value used for r_{ij} will produce an enormous error in τ_R. By combining published crystal structure data for yeast $tRNA^{Phe}$ (Jack et al., 1976; Stout et al., 1978; Sussman et al., 1978) with the N–H bond lengths from the single nucleotide data of Hoogsteen (1968), a useful model of the GU-4 base pair in that tRNA can be made. It seems reasonable to anticipate that the interproton spacing for the imino protons of GU-4 in $tRNA^{Phe}$ will be very similar to the spacing of the imino protons in the GU-50 base pair of *E. coli* $tRNA_1^{Val}$. The interproton spacing that results from our model calculations is 0.233 nm for the Klug crystal structure (Jack et al., 1976), 0.305 nm for the Sundaralingham crystal structure (Stout et al., 1978), and 0.176 nm for the Kim structure (Sussman et al., 1978). Using these values along with $\sigma_{ij} = 2.53\ s^{-1}$ in eq 2 gives rotational relaxation times (after correction to 20 °C in water) of 9.6, 48.7, and 1.8 ns, respectively. None of these values agrees very well with the value of τ_R measured in the FPA experiment. The value of 1.8 ns resulting from the Kim data is clearly far too low and indicates that this structure predicts an interproton spacing that is much too small. The measured value of τ_R is actually bracketed by the values calculated from the Klug and the Sundaralingham structures, implying that the true spacing lies in between these two predictions, i.e., 0.233 nm $< r_{ij} <$ 0.305 nm.

It is perhaps unreasonable to expect to extract precise interproton spacings from the X-ray data, which do not reveal proton positions and in which the accuracy of the other atomic positions is limited by the experimental resolution (~0.17–0.3 nm), so we should turn the problem around. For the first time we have independent measurements of σ_{ij} and τ_R on essentially identical samples and are able to give a very reliable estimate of r_{ij}. It is important to appreciate that, because NOEs depend on the inverse sixth power of the internuclear distance (see eq 2), most of the observed relaxation occurs when the protons are in their position of closest approach. This means that the r_{ij} estimated from NOE experiments is a lower bound value. Using $\tau_R = 17.8$ ns (the measured value at 20 °C scaled to 32 °C) and the cross-relaxation rate given above in eq 2 gives $r_{ij} = 0.272$ nm for the distance between the N1-H of G-50 and N3-H of U-64 in $tRNA_1^{Val}$. The largest uncertainty in this value is associated with the determination of σ_{ij}. However, even if σ_{ij} had an error as high as 25%, our estimate of r_{ij} would have an uncertainty of less than 5%. The present estimate is similar to the value of 0.288 nm estimated by Johnston & Redfield (1981) for the imino–imino distance of the GU-4 base pair in yeast $tRNA^{Phe}$. Since the latter workers did not have an independent measure of τ_R but had to guess a value, the present estimate of $r_{ij} = 0.272$ nm may be considered the more reliable value.

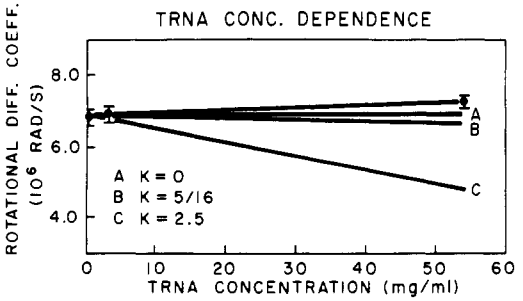

FIGURE 3: Variation of the rotational diffusion coefficient D_R with concentration for $tRNA_1^{Val}$. Ionic strength is 130 mM.

To compare the concentration dependence we observe with that predicted from eq 1, we convert the measured rotational relaxation times to equivalent sphere rotational diffusion coefficients by using

$$D_R = 1/(6\tau_R) \tag{5}$$

These data are shown in Table I and are plotted as a function of concentration in Figure 3. These data are notworthy on two accounts. First, there is surprisingly little variation over the range of concentration studied. Second, D_R may actually *increase* slightly as the tRNA concentration increases. This is contrary to the expectation from eq 1.

Even though the observed change in D_R with tRNA concentration is in the opposite direction to that predicted from eq 1, it is worthwhile to compare the *magnitude* of the observed change with the expected change. The measured D_R may be fitted to a relationship of the form

$$D_R = D_R^0 + K^1 C \tag{6}$$

where C is the tRNA concentration in milligrams per milliliter. This best fit curve is shown drawn through the experimental data in Figure 3. In this case, the zero concentration intercept is

$$D_R^0 = (6.88 \pm 0.17) \times 10^6\ rad^2/s$$

and the slope is

$$K^1 = (6.16 \pm 1.35) \times 10^3$$

We then calculate

$$D_R/D_R^0 = 1 + K^1 C/D_R^0 = 1.05 \pm 0.26 \quad \text{at 54 mg/mL}$$

To compare this with the prediction from eq 1, the tRNA volume fraction ϕ must be estimated. Using $D_R^0 = 6.88 \times 10^6$ rad^2/s, we calculate the equivalent hydrodynamic sphere volume of a tRNA molecule as $V = 98.14 \times 10^{-27}\ m^3$. Assuming $M_r \sim 26000$, the volume fraction at 54 mg/mL is then $\phi = 0.123$. With this value for ϕ, we can calculate the concentration dependence of D_R predicted from eq 1 for the various values of K (2.5, $^5/_{16}$, 0). These predictions are plotted on Figure 3, and it is apparent that none of these faithfully reproduces the observed concentration dependence. For comparison we calculate

$$D_R/D_R^0 = 0.693 \quad \text{for } K = 2.5$$

$$D_R/D_R^0 = 0.962 \quad \text{for } K = {}^5/_{16}$$

$$D_R/D_R^0 = 1.0 \quad \text{for } K = 0$$

The value $K = 2.5$ predicts a 30% change (decrease) in D_R between 0 and 54 mg/mL. This is ~6 times greater than the 5% change (increase) that we observe and is well outside our experimental error. For $K = {}^5/_{16}$, the predicted change is ~4% (decrease), which agrees closely with the magnitude of the observed change. $K = 0$ of course leads to no change in D_R with tRNA concentration. Despite the fact that the statistical error in K^1 is only ~24%, we cannot rule out the possibility of $K = 0$ (i.e., no change in D_R), especially in view of the fact that we only have three data points.

The observation that the concentration dependence of D_R is small and maybe even in the opposite direction to that predicted from eq 1 has two possible explanations. The first (trivial) possibility is that existing theories do not predict the correct value (sign and magnitude) of the coefficient K. The second possibility is that, due to the long-range electrostatic interaction, the tRNA molecules are held sufficiently far apart to reduce significantly the hydrodynamic interaction. The SAXS data of Patkowski et al. (1980) for concentrated (46 mg/mL) tRNA show well-defined maxima even at 60 mM NaCl, suggesting that the solution is substantially ordered. Although it is not known whether such maxima are also present in our solutions with 54 mg/mL in 130 mM ionic strength, it is virtually certain that close approaches of adjacent tRNAs are significantly impeded. The present hydrodynamic theories are based on a random distribution of neighbors and therefore predict a lower D_R than would be expected for a nonrandom distribution with a paucity of very near neighbors.

Patkowski & Chu (1979) have previously concluded that D_R for bulk yeast tRNA has a negligible concentration dependence; however, it is unclear how much weight to give to that conclusion in view of the limited concentration range studied and the quality of the experimental data. Their measurements of D_R were based on depolarized DLS experiments in which data were typically accumulated for 12–24 h (Patkowski et al., 1978). Even then, the signal-to-noise ratio was such that heavy massaging with various smoothing schemes and the total elimination of some data points were necessary to achieve the quoted ±10% uncertainty in D_R. Such an uncertainty means that these authors could not resolve a change in D_R as large as 20%, and since the two tRNA concentrations studied (9.6 and 20.4 mg/mL) differed only by a factor of 2, they are clearly unable to say with any confidence that D_R does not have a concentration dependence. Indeed, D_R could change by as much as 20% as the concentration changes by just a factor of 2! In any event, since DLS experiments measure *mutual* diffusion coefficients whereas FPA measures the *tracer* (or self) diffusion coefficient, it is not clear how the results of Patkowski and Chu compare with the present results.

Effect of Ionic Strength on tRNA at 54 mg/mL. (*a*) *Fluorescence Decay.* From Table II we see that over the range of salt concentrations studies (2–100 mM) the $S(t)$ parameters show little variation and have values very close to those obtained at lower $tRNA_1^{Val}$ concentration and physiological ionic strength (see Table I). The fact that the fluorescence parameters are unchanged indicates that even at 2 mM NaCl the $tRNA_1^{Val}$ is essentially in its native form (or at least the form that prevails under physiological conditions).

(*b*) *Fluorescence Polarization Anisotropy.* A more surprising observation to come out of the data of Table II is that the anisotropy decay parameters show no real dependence on ionic strength over the range 2–100 mM. Indeed, the anisotropy decay times τ_R are equal within experimental error and are close to the value $\tau_R \sim 24$ ns that we obtain for this tRNA under physiological salt conditions (Table I).

The finding that τ_R does not change at low ionic strength is unexpected since at 2 mM NaCl the Debye length $\kappa^{-1} \sim 6.7$ nm and the length of the tRNA (~7.8 nm) are both greater than the mean particle spacing $\zeta_R \sim 5.1$ nm. Under these conditions there must be a strong electrostatic interaction between the molecules. The SAXS data of Patkowski et al. (1980) show pronounced maxima for tRNA in concentrated solution at or below ~12 mM salt, indicating the presence of substantial ordering. Their low-salt Bragg spacing data (Table I; Patkowski et al., 1980) may be linearly extrapolated to a tRNA concentration of 54 mg/mL, giving a spacing of $d_B \sim 6.5$ nm. This value is larger than the mean particle spacing of ~5.1 nm expected for a random distribution of particles at this concentration and is very close to the Debye length given above. It seems that the electrostatic interaction imposes substantial spatial ordering on the tRNA molecules and greatly modifies their translational dynamics, yet the rotational degrees of freedom remain largely unaffected as evidenced by the unchanged values for τ_R.

Conclusions

Using time-resolved FPA techniques, we have demonstrated that the rotational Brownian motion of indivudal tRNA molecules is remarkably insensitive to both nucleic acid concentration and solvent ionic strength. This is in contrast with the dramatic decrease in translational Brownian motion observed by others in concentrated solutions at low ionic strength. Thus, it appears that rotational motion is affected much less severely by electrostatic and hydrodynamic interactions than is translational motion. We should point out though that it is only those techniques that are sensitive to *mutual* diffusion (e.g., DLS) that report anomalous translational diffusion behavior. Techniques that measure *tracer* diffusion (Zero & Ware, 1984; Ware et al., 1983) seem to indicate relatively normal translational mobilities in the case of poly(L-lysine).

It is clear from our results that, in the case of tRNA, even at the high concentrations routinely used in the NMR experiments the macromolecules undergo unimpeded rotational motions. It is therefore legitimate to use rotational relaxation times measured by other techniques at (usually) much lower tRNA concentrations when interpreting NMR data.

By combining time-dependent NOE data with FPA measurements of the rotational relaxation time, we have provided the first reliable estimate of the interproton distance for the G-50 N1-H and U-64 N3-H protons in $tRNA_1^{Val}$. This distance is 0.272 nm.

Acknowledgments

We thank Prof. B. R. Reid for helpful discussions and encouragement and Susan Ribeiro for expert technical assistance and sample preparation. We also thank Kerrie Thomas for typing the manuscript.

References

Bevington, P. R. (1969) *Data Reduction and Error Analysis for the Physical Sciences*, McGraw-Hill, New York.

Bothner-By, A. A. (1979) in *Biological Applications of Magnetic Resonance* (Shulman, R. G., Ed.) p 177, Academic Press, New York.

Chandrasekhar, S. (1943) *Rev. Mod. Phys. 15*, 1.

Cotton, J. P., & Moan, M. (1976) *J. Phys. Lett. 37*, L75.

Crandall, R. S., & Williams, R. (1977) *Science (Washington, D.C.) 198*, 293.

Freed, K. F., & Muthukumar, M. (1978) *J. Chem. Phys. 69*, 2657.
Fullmer, A. W., Benbasat, J. A., & Bloomfield, V. A. (1981) *Biopolymers 20*, 1147.
Giordano, R., Maisano, G., Mallamase, F., Nicali, N., & Wanderlingh, F. (1981) *J. Chem. Phys. 75*, 4770.
Hachisu, S., Kobayashi, Y., & Kose, A. (1973) *J. Colloid Interface Sci. 42*, 342.
Hare, D. R., & Reid, B. R. (1982a) *Biochemistry 21*, 1835.
Hare, D. R., & Reid, B. R. (1982b) *Biochemistry 21*, 5129.
Heerschap, A., Haasnoot, C. A. G., & Hilbers, C. W. (1983) *Nucleic Acids Res. 11*, 4483.
Hoogsteen, K. (1968) in *Molecular Associations in Biology* (Pullman, B., Ed.) p 21, Academic Press, New York.
Ise, N., & Okubo, T. (1980) *Acc. Chem. Res. 13*, 303.
Ise, N., Okubo, T., Yamamoto, K., Kawai, H., Hashimoto, T., Fujimura, M., & Miragi, Y. (1980) *J. Am. Chem. Soc. 102*, 7901.
Ise, N., Okubo, T., Sugimura, M., Ito, K., & Nolte, H. J. (1983a) *J. Chem. Phys. 78*, 536.
Ise, N., Okubo, T., Yamamoto, K., Matsuoka, H., Kawai, H., Hashimoto, T., & Fujimura, M. (1983b) *J. Chem. Phys. 78*, 541.
Jack, A., Ladner, J. E., & Klug, A. (1976) *J. Mol. Biol. 108*, 619.
Johnston, P. D., & Redfield, A. G. (1978) *Nucleic Acids Res. 5*, 3913.
Johnston, P. D., & Redfield, A. G. (1981) *Biochemistry 20*, 1147.
Kose, A., Ozaki, M., Takano, K., Kobayashi, Y., & Hachisu, S. (1973) *J. Colloid Interface Sci. 44*, 330.
Lee, W. I., & Schurr, J. M. (1975) *J. Polym. Sci., Polym. Phys. Ed. 13*, 873.
Liebmann, M., Rubin, J., & Sundaralingham, M. (1977) *Proc. Natl. Acad. Sci. U.S.A. 74*, 4821.
Lin, S. C., Lee, W. I., & Schurr, J. M. (1978) *Biopolymers 17*, 1041.
Maret, G., Domard, A., & Rinaudo, M. (1979) *Biopolymers 18*, 101.
Martin, N. B., Tripp, J. B., Shibata, J. H., & Schurr, J. M. (1979) *Biopolymers 18*, 2127.
Moan, M. (1978) *J. Appl. Crystallogr. 11*, 519.
Moan, M., & Wolff, C. (1975) *Polymer 16*, 776.
Moan, M., Wolf, C., & Ober, R. (1975) *Polymer 16*, 781.
Moan, M., Wolff, C., Cotton, J. P., & Ober, R. (1979) *J. Polym. Sci., Polym. Symp. 61*, 1.
Montgomery, J. A., & Berne, B. J. (1977) *J. Chem. Phys. 67*, 4589.
Nierlich, M., Williams, C. E., Boué, F., Cotton, J. P., Daoud, M., Farnoux, B., & Jannink, G. (1978) *J. Appl. Crystallogr. 11*, 504.
Nierlich, M., Williams, C. E., Boué, F., Cotton, J. P., Daoud, M., Farnoux, B., Jannink, G., Picot, C., Moan, M., Wolff, C., Rinaudo, M., & de Gennes, P. G. (1979) *J. Phys. (Orsay, Fr.) 40*, 701.
Ohtsuki, T., Mitaku, S., & Okano, K. (1978) *Jpn. J. Appl. Phys. 17*, 305.
Patkowski, A., & Chu, B. (1979) *Biopolymers 18*, 2051.
Patkowski, A., Jen, S., & Chu, B. (1978) *Biopolymers 17*, 2643.
Patkowski, A., Gulari, E., & Chu, B. (1980) *J. Chem. Phys. 73*, 4178.
Plestil, J., Mikes, J., & Dusek, K. (1979) *Acta Polym. 30*, 29.
Reid, B. R., Ribeiro, N. S., McCollum, L., Abbate, J., & Hurd, R. E. (1977) *Biochemistry 16*, 2086.
Rinaudo, M., & Domard, A. (1977) *J. Polym. Sci., Polym. Lett. Ed. 15*, 411.
Schaefer, D. W., & Ackerson, B. J. (1976) *Phys. Rev. Lett. 35*, 1448.
Schmitz, K. S. (1982) *Biopolymers 21*, 1383.
Schmitz, K. S., Parthasarathy, N., Kent, J. C., & Gauntt, J. (1982) *Biopolymers 21*, 1365.
Schmitz, K. S., Lu, M., & Gauntt, J. (1983) *J. Chem. Phys. 78*, 5059.
Shibata, J. H., & Schurr, J. M. (1979) *Biopolymers 18*, 1831.
Southwick, J. G., Jamieson, A. M., & Blackwell, J. (1981) *Macromolecules 14*, 1728.
Stout, C. D., Mizuno, H., Rao, S. T., Swaminanathan, P., Rubin, J., Brennan, T., & Sundaralingham, M. (1978) *Acta Crystallogr., Sect. B. B34*, 1529.
Sussman, J. L., Holbrook, S. R., Warrant, R. W., Church, G. M., & Kim, S.-H. (1978) *J. Mol. Biol. 123*, 607.
Takano, K., & Hachisu, S. (1977) *J. Chem. Phys. 67*, 2604.
Tao, T. (1969) *Biopolymers 8*, 609.
Tao, T., Nelson, J. H., & Cantor, C. R. (1970) *Biochemistry 9*, 3514.
Thomas, J. C., & Schurr, J. M. (1983) *Biochemistry 22*, 6194.
Thomas, J. C., Allison, S. A., Appellof, C. J., & Schurr, J. M. (1980) *Biophys. Chem. 12*, 177.
Thomas, J. C., Schurr, J. M., Reid, B. R., Ribeiro, N. S., & Hare, D. R. (1984) *Biochemistry* (following paper in this issue).
Ware, B. R., Cyr, D., Gorti, S., & Lanni, F. (1983) in *Measurement of Suspended Particles by Quasi-Elastic Light Scattering* (Dahneke, B. E., Ed.) p 255, Wiley-Interscience, New York.
Wells, B. D., & Cantor, C. R. (1980) *Nucleic Acids Res. 8*, 3229.
Wilcoxon, J. P., & Schurr, J. M. (1983) *J. Chem. Phys. 78*, 3354.
Williams, R., & Crandall, R. S. (1974) *Phys. Lett. 484*, 225.
Williams, R., Crandall, R. S., & Wojtowicz, P. J. (1976) *Phys. Rev. Lett. 37*, 348.
Williams, C. E., Nierlich, M., Cotton, J. P., Jannink, G., Boué, F., Daoud, M., Farnoux, B., Picot, C., de Gennes, P. G., Rinaudo, M., Moan, M., & Wolff, C. J. (1979) *J. Polym. Sci., Polym. Lett. Ed. 17*, 379.
Wolynes, P. G., & Deutch, J. M. (1977) *J. Chem. Phys. 67*, 433.
Zero, K., & Ware, B. R. (1984) *J. Chem. Phys. 80*, 6110.